Available online at www.sciencedirect.com

ScienceDirect

Advances in Space Research 55 (2015) 630–638

ADVANCES IN SPACE RESEARCH (a COSPAR publication)

www.elsevier.com/locate/asr

Impacts of tug and debris sizes on electrostatic tractor charging performance

Erik A. Hogan *, Hanspeter Schaub

University of Colorado at Boulder, Boulder, CO 80309, United States

Received 6 June 2014; received in revised form 17 October 2014; accepted 21 October 2014
Available online 25 October 2014

Abstract

Active debris removal techniques enable relocating noncooperative geosynchronous (GEO) debris objects into graveyard orbits. One proposed method is the electrostatic tractor concept. Here a tug vehicle approaches a target debris object and emits an electron beam onto the debris. The charging that results yields an attractive electrostatic force that is used to tow the debris object into a new orbit. In this study, the impacts of relative sizing between tug and debris on the efficacy of this charge transfer process are considered. By applying a charging model and incorporating nominal, quiet GEO space weather conditions, limitations on the size ratio that preclude charge transfer are identified for different levels of beam energy. The resulting electrostatic forces and impacts on reorbiting performance are studied. The results indicate that a larger tug vehicle will enable the tugging of a broader range of debris sizes, and that the tug size should be roughly as large as the expected debris size.

Keywords: Electrostatic tractor; Spacecraft charging; Active charge transfer; Active debris removal

1. Introduction

For GEO satellites, international guidelines for end-of-life operations call for removal of the spacecraft from the GEO region. With a goal of preventing reentry into GEO within 25 years, a minimum increase in altitude of 200–300 km is typically expected, though certain spacecraft may be raised higher (IADC, 2007; NASA, 1995). For the case of defunct satellites and other debris objects, a method is needed for achieving this transition into a graveyard orbit. To that end, the use of an electrostatic tractor, illustrated in Fig. 1, has been proposed (Schaub and Moorer, 2012). A tug vehicle approaches a target object and emits an electron beam onto the debris, charging it negatively. With the beam emission resulting in a positive charge on the tug, an attractive electrostatic force between the tug and debris results, which is then used in conjunction with low thrust to tow the debris object into a disposal orbit (Hogan and Schaub, 2013). The charging that results is dependent on several current sources, and is impacted by the variations in the space weather environment at GEO (Denton et al., 2005; Schaub and Sternovský, 2013; Hogan and Schaub, 2014).

Due to the potential impacts of spacecraft charging on operations and spacecraft lifetime, much work has been performed in this area (Garrett, 1981; DeForest, 1972; Mullen et al., 1986; Katz et al., 1998; Cho et al., 2012; Anderson, 2012). Typically, these studies focus on a single satellite in orbit and investigate natural charging events that occur as a result of the space weather environment. A serious concern for spacecraft that experience differential charging across their outer surface is electrostatic discharge (ESD) events, where arcing occurs between different substructures possessing a significant surface potential

* Corresponding author.
E-mail addresses: erik.hogan@colorado.edu (E.A. Hogan), hanspeter.schaub@colorado.edu (H. Schaub).

http://dx.doi.org/10.1016/j.asr.2014.10.023
0273-1177/

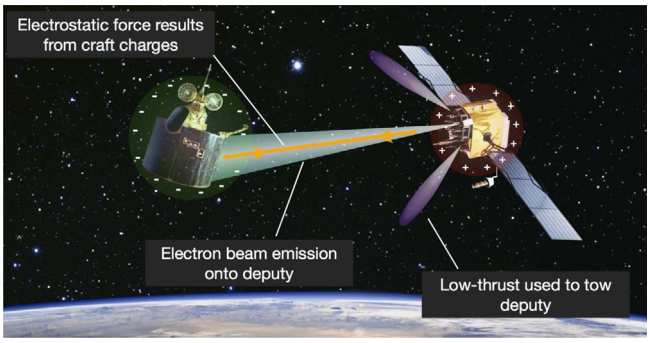

Fig. 1. Electrostatic tractor concept.

difference (Katz et al., 1998). These ESD events can be destructive to electronic hardware. Recent studies indicate that large satellites in GEO may experience many thousands of discharges over their lifetimes (Cho et al., 2012). With the electrostatic tug concept, the electron beam is used to raise the absolute potential of the vehicle, and thus avoids the differential charging issues. Current GEO spacecraft construction practice ensures that all outer surfaces are interconnected, thus minimizing differential charging issues. For electrostatic tugging, potential levels on the order of tens of kiloVolts are required (Schaub and Jasper, 2013). While certainly the near proximity of highly charged spacecraft raises a concern of potential arcing between tug and debris, in GEO arcing occurs over distances of a few centimeters for kiloVolt levels of potential difference (Cho et al., 2003). This is many times smaller than the separation distances considered, so arcing between tug and debris is not a concern.

Due to the recent nature of the electrostatic tractor concept, limited work has been performed in modeling the charge transfer process. In Schaub and Sternovský (2013), a charging model is developed to predict the potentials on tug and debris as a function of electron beam emission, spacecraft properties, and the space environment. A similarly sized tug and debris object are considered, and the charges are computed for a single space weather condition. Hogan and Schaub (2014) investigates the charge transfer process further, considering the impacts that fluctuations in the GEO plasma conditions over a typical day have on tractor performance. Modifying the beam current to counter varying conditions is contrasted with simply maintaining a constant current, and a simulation is used to illustrate a reorbiting maneuver. Once again, a single size is chosen for the debris object and tug, with the debris object roughly half the size of the tug. Thus far, the question of whether or not a tug could successfully tow a much larger object has not been investigated.

In this study, the impacts of relative size between the tug vehicle and debris object are considered. Because several of the currents impacting charging are dependent on spacecraft surface area, it is possible that sufficient charging may not occur if there is a significant size difference between tug vehicle and debris object. In order to charge a debris object to the kiloVolt levels considered for tugging, a large enough portion of the electron beam current must reach it in order to overcome the various currents it is subjected to. If the tug vehicle emitting the electron beam is small enough relative to the debris object, it will charge completely (referred to here as supercharging) and prevent sufficient beam current from reaching the debris. The amount of current that can be emitted by the tug is limited by the beam energy. Once the tug potential reaches the level of the beam energy, any additional beam current will be recollected by the tug (Lai, 2012). The impacts of size differences on the resulting charging are studied, with hopes of identifying a threshold for the onset of charging. The electrostatic forces and reorbiting performance for different sizing configurations are also considered.

The paper is structured as follows. First, an overview of the charging process and the model used to compute the potentials on tug and debris objects is presented. This is followed by a brief explanation of the method used to compute the electrostatic forces between tug and debris. Next, a threshold for the onset of charge transfer is defined, and the impacts of relative sizing on meeting this threshold are investigated. Then, the electrostatic forces acting between tug and debris are studied for a range of sizes and charging conditions. Lastly, the impacts of relative sizing on the debris reorbiting performance are considered for a range of tugging configurations, and power requirements are determined.

2. Background

In this paper, it is assumed that the tug vehicle is equipped with an electron gun that is used to remotely charge a neighboring deputy (or debris) object up to 10s of meters away. The charge transfer, in combination with the near proximity of tug and deputy, results in an attractive electrostatic force used for tugging, as illustrated in Fig. 1. Here, the problem of reorbiting a GEO debris object into a graveyard orbit is considered. A semi-major axis change is required and the tug and deputy maintain a constant leader–follower position throughout the duration of the maneuver (Hogan and Schaub, 2013; Schaub and Jasper, 2013). The study utilizes a charging model that accounts for the numerous current sources experienced by a satellite in the space environment. It is assumed that both the tug and deputy are conductive, with spherical geometries. While typical spacecraft do not necessarily satisfy these assumptions, the following analysis is used to provide first-order insight into the limitations of relative sizing between tug and deputy, and identify trends that would extend to more general spacecraft models.

2.1. Spacecraft charging model

The electrostatic tugging force used for towing is a function of the charging that results from the charge transfer between tug and deputy. Several factors influence this

charging process. In the space environment the tug and deputy collect plasma electron and ion currents, and photoelectrons may be emitted depending on the spacecraft potential and presence of sunlight. Charge control is achieved through focused electron beam emission by the tug. When the electron beam is absorbed by the deputy, secondary electron emission occurs as the incoming beam electrons excite and release electrons from the deputy surface material. The potential levels achieved by the tug and deputy result from a balance of these various current sources. To compute these potentials, the charging model developed in Schaub and Sternovský (2013) is applied.

When either spacecraft is in the sunlight, a photoelectron current occurs. This current is modeled by (Lai, 2012)

$$I_{ph}(\phi) = j_{ph,0} A_\perp e^{-\phi/T_{ph}} \quad \phi > 0 \tag{1a}$$

$$= j_{ph,0} A_\perp \quad \phi \leqslant 0 \tag{1b}$$

where ϕ is the spacecraft potential, $T_{ph} = 2$ eV is the temperature of the emitted photoelectrons, $j_{ph,0} = 20\ \mu\text{A/m}^2$ is the photoelectron flux, and $A_\perp$ is the cross-sectional area exposed to sunlight. For the spherical geometries assumed here, $A_\perp = \pi r^2$. For high positive potentials, the photoelectron current is effectively zero because all of the emitted electrons are recaptured.

The plasma electron current is modeled by Pfau and Tichy (2001)

$$I_e(\phi) = -\frac{A q n_e w_e}{4} e^{\phi/T_e} \quad \phi < 0 \tag{2a}$$

$$= -\frac{A q n_e w_e}{4}\left(1 + \frac{\phi}{T_e}\right) \quad \phi \geqslant 0 \tag{2b}$$

where $A = 4\pi r^2$ is the surface area exposed to the plasma environment, q is the elementary charge, n_e is the plasma electron density, T_e is the plasma electron temperature, and $w_e = \sqrt{8T_e/\pi m_e}$ is the thermal velocity of the electrons. The electron mass is represented by m_e. Note that for large negative potentials, I_e is very small. This is due to the fact that electrons are repelled by the negatively charged spacecraft.

The plasma ion current is modeled as (Pfau and Tichy, 2001)

$$I_i(\phi) = \frac{A q n_i w_i}{4} e^{-\phi/T_i} \quad \phi > 0 \tag{3a}$$

$$= \frac{A q n_i w_i}{4}\left(1 - \frac{\phi}{T_i}\right) \quad \phi \leqslant 0 \tag{3b}$$

which is very similar in form to the plasma electron current. Here, $w_i = \sqrt{8T_i/\pi m_i}$ is the thermal velocity of the ions. Additional variable quantities are defined as before, except the subscript i is used to denote they represent ions. In the space weather model for the GEO environment utilized here, the ion species consists solely of protons. For high positive potentials, the ion current is very small because the ions are repelled by the positively charged spacecraft.

Control of the tug and deputy potentials is achieved through electron beam emission from the tug onto the deputy. Depending on the charge levels of tug and deputy, as well as beam pointing accuracy, some fraction of the beam current will be absorbed by the deputy. This current is modeled as

$$I_D(\phi_D) = -\alpha I_t \quad q\phi_T - q\phi_D < E_{EB} \tag{4a}$$

$$= 0 \quad q\phi_T - q\phi_D \geqslant E_{EB}, \tag{4b}$$

where I_t is the beam current emitted by the tug, E_{EB} is the electron beam energy, and the subscripts T and D represent the tug and deputy, respectively. The parameter α is the fraction of the beam current emitted by the tug that is absorbed by the deputy and is analogous to the efficiency of the charge transfer process. In the current paper a value of $\alpha = 1$ is used, which maintains the standard established in Schaub and Sternovský (2013). This assumes a well focused and accurately pointed beam, and better quantification of α is beyond the scope of this paper. Once $q\phi_T - q\phi_D = E_{EB}$, it is impossible for additional beam current to make it to the deputy. The emitted beam electrons do not have enough energy to cross the potential difference between tug and deputy.

The incoming beam electrons absorbed by the deputy give rise to emitted secondary electrons. These electrons will be lost, owing to the large negative potential on the deputy. This current source is significant and must be included in the computation of the deputy potential. Secondary electron emission is modeled by Draine and Salpeter (1979)

$$I_{\text{SEE}}(\phi_D) = -4Y_M I_D(\phi_D)\kappa \quad \phi_D < 0 \tag{5a}$$

$$= 0 \quad \phi_D \geqslant 0, \tag{5b}$$

where

$$\kappa = \frac{E_{\text{eff}}/E_{\max}}{\left(1 + E_{\text{eff}}/E_{\max}\right)^2}$$

and $E_{\text{eff}} = E_{EB} - q\phi_T + q\phi_D$. Y_M is the maximum yield of secondary electron production, and $E_{\max}$ is the impact energy at which this maximum occurs. In this paper, the values of $Y_M = 2$ and $E_{\max} = 300$ eV are used, maintaining the values established in Reference Schaub and Sternovský (2013). While metallic materials typically have a yield in the neighborhood of 1, the maximum yield of secondary electron production may differ by a factor of 2 for spherical objects due to isotropic incidence (Draine and Salpeter, 1979). This is the reason why a value of $Y_M = 2$ is chosen.

Because the tug will be charged to high positive potentials, the tug charging is dominated by the electron beam emission and plasma electron currents. The tug settles to a potential that satisfies the simplified current balance $I_e(\phi_T) + I_t = 0$, which is analytically solved as follows:

$$\phi_T = \left(\frac{4I_t}{A q n_e w_e} - 1\right) T_e. \tag{6}$$

The current balance on the deputy object contains a few more contributions, and typically a numerical root finder

must be used to obtain a solution. The deputy potential must satisfy

$$I_e(\phi_D) + I_i(\phi_D) + I_{\mathrm{SEE}}(\phi_D) + I_{ph}(\phi_D) + I_D(\phi_D) = 0. \quad (7)$$

The presence of the photoelectron current implies the deputy is in the sunlight. If this is not the case, the current balance is modified so that it no longer contains I_{ph}.

It is assumed that the potentials ϕ_T and ϕ_D that result from this charging model are absolute potentials (Sickafoose et al., 2002), and that the plasma electron and ion currents are functions of the background plasma densities. However, the plasma distribution in the presence of a highly charged object is perturbed. For example, in the vicinity of the positively charged tug, the electron density will be higher than background, and the ion density will be lower. Even though the deputy is located within this region, the background densities are used in the electron and ion current expressions. The strength of this assumption is not clear at this time, and future work is needed to investigate and possibly modify the charging model. If it is found that the redistribution of electron and ions affects the charging currents significantly, the charging model used here would not be valid. This could result in significant changes to the results presented in this paper.

In the event that the tug cannot deliver electron beam current to the deputy, the charging model will yield a deputy potential that is a function of the plasma ion and electron currents and the photoelectron current. The charging is dominated in large part by the photoelectron current, which is of higher magnitude than the plasma currents. Because of this, the charging model will result in a deputy potential of a few volts positive due to emission of photoelectrons. When the deputy reaches this slightly positive potential, photoelectrons are recaptured and the deputy reaches equilibrium potential.

The highly charged nearby tug, however, changes this dynamic somewhat. In isolation, the deputy begins recollecting photoelectrons at only a few volts positive. This is reflected in Eq. (1a) where the net photoelectron current decays to zero as the deputy is charged to higher potentials. Essentially, the reason why the deputy settles to a few volts positive is because this is the potential at which a large portion of the emitted photoelectrons are recaptured. With the tug nearby at a high positive potential, emitted photoelectrons will be collected by the tug because the electric field in the vicinity of the deputy will point away from it, even if the deputy is at a few volts positive. At low positive potentials, the photoelectrons will not be recaptured by the deputy. This loss of negative charge (outgoing electrons) will raise the deputy potential until the deputy begins recapturing enough photoelectrons to result in a net zero current. This phenomenon is not captured by the charging model here, and so the charging model cannot be applied to the case when charge transfer does not occur. When charge transfer occurs, driving the deputy to a negative potential, there is enough electron beam current to offset the loss of photoelectrons and this issue is not a problem. Modifying the charging model for applicability to the non-charge transfer scenario would be a good area for future work.

2.2. Electrostatic force modeling

The electrostatic tractor takes advantage of the attractive electrostatic force generated between the tug and deputy. Due to the various current sources detailed previously, the tug and deputy will achieve voltages of ϕ_T and ϕ_D, respectively. These are absolute potentials, as opposed to a potential relative to the plasma environment (Sickafoose et al., 2002). In order to compute the resulting electrostatic force, a relationship is needed between the potentials and charges for the spacecraft. Here, a position dependent capacitance model is used (Schaub and Jasper, 2013; Static, 1968; Slisko and Brito-Orta, 2007). The voltage and charges on the tug and deputy are related through

$$\begin{bmatrix} \phi_T \\ \phi_D \end{bmatrix} = k_c \begin{bmatrix} \frac{1}{r_T} & \frac{1}{L} \\ \frac{1}{L} & \frac{1}{r_D} \end{bmatrix} \begin{bmatrix} q_T \\ q_D \end{bmatrix}, \quad (8)$$

where L is the separation distance between tug and deputy, $k_c = 8.99 \times 10^9\ \mathrm{Nm^2/C^2}$ is Coulomb's constant, r_T and r_D are the radii of tug and debris, respectively, and q_T and q_D are the charges on tug and deputy, respectively.

Once ϕ_D and ϕ_T are computed using the current balances detailed above, Eq. (8) is inverted to solve for the charges. The electrostatic force is then computed using

$$F_e = k_c \frac{q_T q_D}{L^2}. \quad (9)$$

This force acts equally and opposite on the tug and deputy, and its direction is dependent on the relative position between the two objects. A positive value signifies a repulsive force, while a negative value represents an attractive force.

The space plasma environment will partially shield the electrostatic force. The distance over which this shielding occurs is characterized by the plasma Debye length (Bittencourt, 2004). The nominal GEO space weather conditions considered here have Debye lengths of a few tens of meters, which is on the order of the electrostatic tractor separation distances. This is characteristic of quiet solar activity conditions, where there is an upflow of colder ions from the ionosphere (Denton et al., 2005). This actually provides the worst-case charging performance, because these colder ions mitigate the charging on the deputy to a certain degree. Because of the high potential levels obtained by tug and deputy, the Debye shielding effect will be several times smaller than predicted by the standard Debye length calculation. As discussed in Murdoch et al. (2008) and Stiles et al. (2012), objects charged to high enough potentials in the space environment experience effective Debye lengths several times larger. In the quiet GEO space weather conditions used in this study, only several tens of Volts are required to yield larger effective Debye lengths than predicted with classical Debye–Hückel theory (Stiles et al., 2012). Thus, the space weather condi-

tions are not expected to provide any significant shielding for the separation distances considered (15 m or less). For this reason, the Debye shielding terms are not included in the electrostatic force model.

3. Relative sizing considerations

The maximum allowable electron beam current is driven by the energy of the beam. If enough current is emitted, the tug will achieve a potential equal to the beam energy. Beyond this limit, any emitted beam electrons will be captured by the tug because they do not have enough energy to escape the tug potential well. This has important implications regarding the relative sizing between tug and deputy that will still permit charge transfer. If the tug vehicle is much smaller than the deputy, the tug will reach its potential limit before it has emitted enough current to charge the deputy. This will significantly hinder performance if the sizing difference is large enough. Thus, it is of interest to identify how large a tug vehicle must be to tow a deputy object of a given size.

3.1. From a deputy potential perspective

To identify the conditions under which charge transfer is no longer possible, a threshold condition must be defined. Here, ϕ_c is used to represent a cutoff deputy potential. Any scenario that yields a deputy potential below ϕ_c is no longer considered as a case of successful charge transfer. Note that a failure to achieve charge transfer will result in drastically reduced performance. Without a sufficient absorbed beam electron current, the deputy will result in a high positive potential due to the loss of photoelectrons. Because the charging model is not applicable to this scenario, however, performance results for this condition are ignored. It should be noted that selection of ϕ_c is somewhat arbitrary. Here, it is desired to identify a cutoff potential that constitutes significant charging. To do so, natural charging events are used as a guideline. In GEO, spacecraft spend a majority of their time in sunlight, with brief eclipse periods occurring for no more than an hour each day a few weeks before and after an equinox. The ATS-5 mission observed a maximum potential in the sunlight of -300 V, with potentials between -50 and -300 V occurring several times (DeForest, 1972). All of these charging events occurred during periods of very high solar activity, and occurred between local midnight and dawn. The SCATHA satellite was also used to study natural charging in sunlight, and recorded potentials as high as -740 V (Mullen et al., 1986). Considering these natural charging levels, the value of ϕ_c is chosen as -1 kV.

The severity of geomagnetic storms is classified using the k_p index, which is based on the observed variation in the degree of irregular magnetic activity throughout each day, observed at various ground stations (Bartels et al., 1939). The k_p index utilizes an integer scale ranging from 0 to 9, and values of 5 and up indicate that a geomagnetic storm is occurring. For the following analysis quiet ($k_p = 1.5$) space weather conditions at a local time of 17:30 are used, with values of $n_e = 0.47\ \text{cm}^{-3}$, $T_e = 1180$ eV, $n_i = 11\ \text{cm}^{-3}$, $T_i = 50$ eV (Denton et al., 2005). Note that stronger geomagnetic storm activity results in a population of higher energy particles, and more severe natural charging. However, severe storm conditions are not prevalent in GEO, and over the long electrostatic tractor reorbiting times of several months, more quiet conditions prevail.

First, a relationship between emitted beam current and beam energy required to achieve charge transfer is considered for a range of tug and deputy sizes. That is, given a particular ratio of tug and deputy sizes and an emitted beam current, what beam energy E_c would be required to yield ϕ_c? If the actual beam energy is below E_c, then charge transfer is not possible. If the beam energy is above E_c, then charge transfer is possible and deputy potentials above ϕ_c are achievable. Using a numerical root finder, the critical values of E_c are computed for tug sizes of 1 and 2 m as a function of emitted current and the ratio of deputy and tug radii, r_D/r_T. The charging threshold is defined as $\phi_c = -1$ kV. The results are shown in Fig. 2, and several interesting conclusions can be drawn. First, for any given beam energy E_c, there is an upper limit on the deputy size for which charge transfer is possible. For example, considering the $E_c = 40$ keV contour has its outermost edge at roughly $r_D/r_T = 1.2$ (see Fig. 2), any deputy size beyond 1.2 times that of the tug would preclude charge transfer. From a vehicle design perspective, this implies that for better performance a larger tug vehicle should be used. If the tug vehicle is as large or larger than the biggest expected deputy object, then charge transfer will be possible. However, a smaller tug vehicle is limited in the variety of potential deputy candidates that may be towed. There is a tradeoff that must be considered, however, because a larger tug vehicle requires more current to reach the same potential levels. More current requires more power. Thus, while a larger vehicle can potentially tow a wider range of deputy objects, it will require more power to do so.

Another interesting result shown in Fig. 2 is the existence of a hard cutoff in the charging threshold, where higher beam energies no longer allow for the charging of larger deputy objects. It would seem that this might be a function of the size ratio r_D/r_T. However, this cutoff is merely a reflection of the fact that there is some minimum current required to balance the photoelectron and plasma ion currents and reach ϕ_c. An analytic expression for the cutoff is found by considering the limit of very large beam energies ($E_{EB} \to \infty$). While perhaps not practically realistic, computing this limit allows one to identify the minimum theoretical current that is required to accomplish charge transfer for a deputy object of a given size. In the limit of a very large beam energy, the secondary electron emission current is effectively zero, due to the fact that

$$\lim_{E_{EB}\to\infty} \kappa = 0.$$

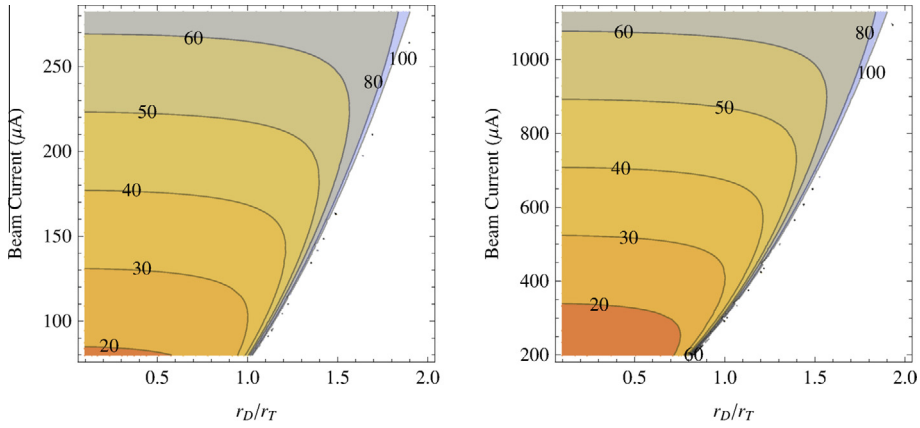

(a) $r_T = 1$ m (b) $r_T = 2$ m

Fig. 2. Beam energy (E_c, in keV) required to reach charging threshold of $\phi_c = -1$ kV for a variety of emitted beam currents and size ratios.

Thus, the current balance on the deputy may be rewritten as

$$I_e(\phi_c) + I_i(\phi_c) + I_{ph}(\phi_c) + I_D(\phi_c) = 0, \tag{10}$$

which can be solved for I_t. Denoting $\mathcal{F}_e = qn_e w_e/4$ and $\mathcal{F}_i = qn_i w_i/4$ as the plasma electron and ion fluxes, the minimum beam current required to achieve ϕ_c is computed as

$$I_{t,c} = \left(4\mathcal{F}_i\left(1 - \frac{\phi_c}{T_i}\right) - 4\mathcal{F}_e e^{\phi_c/T_e} + j_{ph,0}\right)\pi r_D^2. \tag{11}$$

A tug vehicle that cannot emit at least this amount of current, no matter how high the beam energy, will not be able to achieve charge transfer. A plot of $I_{t,c}$ for $\phi_c = -1000$ V is shown in Fig. 3. For finite beam energies, secondary electron emission contributes additional losses to the charge transfer process. More current than predicted in Eq. (11) is required to achieve charge transfer, and the beam energy must be high enough so that the total secondary electron yield is less than one. That is, the number of secondary electrons emitted for every incoming beam electron must be lower than one. If the secondary electron yield is higher than one, then more electrons will be emitted by the deputy than are absorbed from the beam. If this occurs, it is impossible to charge the deputy negative because the net current onto it will be positive due to the net loss of electrons. Depending on the parameters of particular case, the actual current required to achieve charging could be much higher than predicted by $I_{t,c}$.

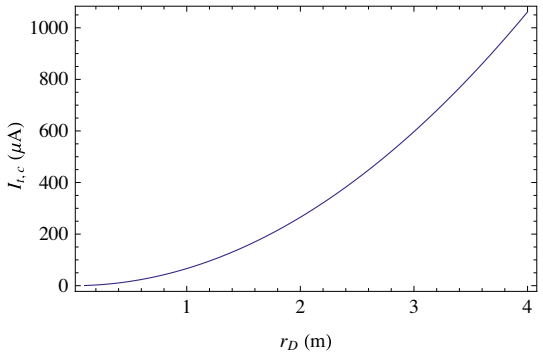

Fig. 3. Minimum current required for charge transfer in the limit of $E_{EB} \to \infty$, assuming a threshold of $\phi_c = -1000$ V.

Returning to Fig. 2, the upper limit on the scaling parameter (r_D/r_T) for a given beam energy is consistent between the two plots. For example, for the 40 keV contour the maximum size ratio for which charge transfer can still be accomplished is roughly 1.2. The primary difference between the two cases where $r_T = 1$ m and $r_T = 2$ m is the amount of current required to reach this peak. The increased current for the larger object sizes is required to offset the higher plasma and photoelectron currents that result from increased surface areas. While it is difficult to determine an expression for the maximum size ratio that still permits charge transfer, the peaks can be computed numerically. To investigate the sensitivity of the upper limits to the tug size, the maximum allowable size ratios are computed for a range of tug radii. The results for beam energies of 20, 40, and 60 keV are shown in Fig. 4(a). It is clear that the upper limits on the relative sizes are not sensitive to the tug size, but rather to the beam energy. A higher beam energy allows for charge transfer onto a larger object. The upper limits on the size ratio for a range of beam energies is shown in Fig. 4(b). At the lower end of the spectrum, a tug vehicle equipped with a 20 keV electron beam would only be capable of achieving charge transfer onto an object roughly three-quarters of its size or smaller. To achieve charge transfer onto a similarly sized object ($r_T = r_D$), the tug vehicle would need an electron beam in excess of 30 keV. As the beam energy increases, larger and larger objects can be charged. This is reflective of the fact that higher beam energies allow the tug vehicle to emit more current before it achieves charge saturation ($q\phi_T = E_{EB}$). Larger deputy objects require more current for charging, as reflected in Fig. 3. Increasing the beam energy allows the tug to provide these higher currents for larger deputy objects.

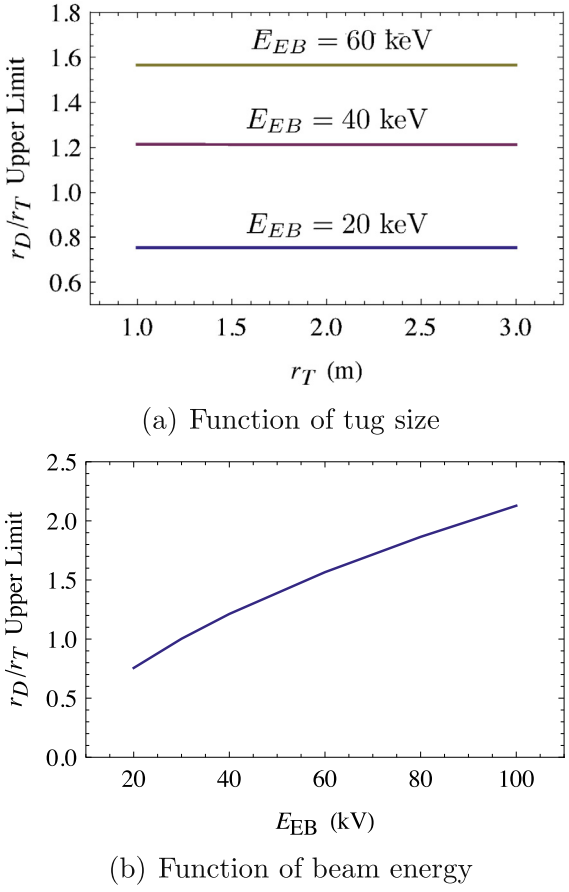

Fig. 4. (a) Size ratio limits for a variety of tug sizes and (b) size ratio limits as a function of beam energy for which charge transfer ($\phi_c - 1$ kV) is possible.

From the perspective of achieving charge transfer, the results thus far suggest that a larger tug is better. A larger tug achieves charge transfer for a wider range of deputy object sizes while requiring less beam energy than a smaller tug. With a 40 keV electron beam, a tug vehicle with a 3 m radius can perform charge transfer onto a deputy object with a radius in excess of 3.5 m. A one-meter tug similarly equipped could only perform charge transfer on an object with a 1.2 m radius. It is important to note that the results shown here are computed for the specific space weather conditions encountered at 17:30 for quiet solar conditions ($k_p = 1.5$). This particular time of day is chosen because it represents the lower end of charge transfer performance, where the electron density is lowest and the ion density is highest. While different space weather conditions would certainly lead to different results, in general the performance would be better than obtained for these particular space weather parameter values.

3.2. From a force perspective

The charge transfer analysis for varying sizes has thus far only been concerned with achieving a potential on the deputy object. However, this is really only part of the bigger picture when it comes to assessing electrostatic tractor performance. The tractor performance is dependent on the electrostatic force that exists between tug and deputy. To illustrate the impact of relative sizing on the resulting electrostatic force, a 2 m tug radius is considered with a beam energy of $E_{EB} = 40$ keV. The electrostatic force magnitudes (in mN) are computed for a range of deputy sizes and beam currents. The results are shown in Fig. 5. The upper limit on the current range is chosen as the condition that provides a tug potential equal to the beam energy ($q\phi_T = E_{EB}$). Additional current emission is not possible, because the beam electrons would be recaptured by the tug.

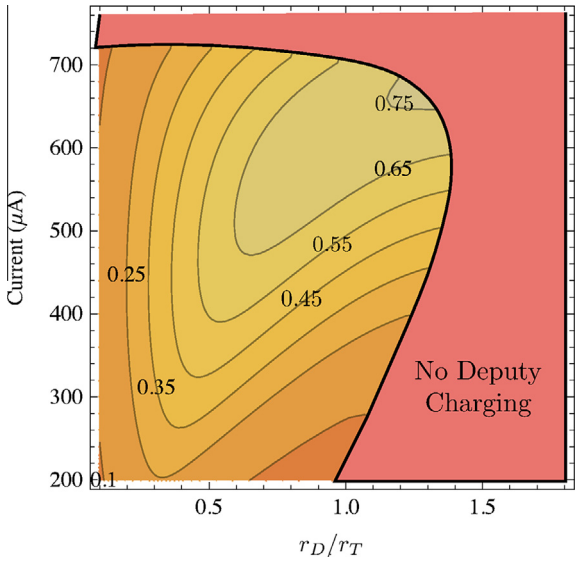

Fig. 5. Electrostatic force magnitude (in mN) for a range of beam currents and deputy sizes, assuming a tug radius of 2 m.

There are two distinct regions on the plot: conditions where charge transfer occurs and a force is computed, and conditions that prevent charge transfer. Where charge transfer fails, the charging model is insufficient to provide a potential on the deputy and a force cannot be computed. Considering the boundary of the region of charge transfer, the largest sized object that can be towed is about 1.35 times the size of the tug. The largest objects enable the largest electrostatic forces. This is due to higher capacitance for larger objects, where more charge exists on the deputy for a given potential. Note that the size ratio of 1.35 is larger than the maximum size ratio (1.2) for charge transfer identified earlier. This is due to the fact that a cutoff potential of $\phi_c = -1$ kV is chosen as a threshold for significant charge transfer. Technically, charge transfer is still occurring when the deputy reaches a potential smaller than ϕ_c, and an electrostatic force still exists, even as the deputy potential approaches zero. This is the reason for the discrepancy between the maximum sizing ratios identified for towing and charge transfer.

3.3. From an orbit raising perspective

Computing the electrostatic force magnitudes only tells half of the story. Larger objects tend to produce larger

forces for a given potential, because the total charge on the objects increases linearly with radius. But larger objects also tend to be heavier, meaning they may be accelerated more slowly. Ultimately, the most important performance criteria that may be considered for the electrostatic tractor is the rate at which the deputy orbit may be changed. Returning to the debris reorbiting scenario, where the objective is increasing the deputy radius by approximately 300 km, the semi-major axis increase over one day is used to quantify the tugging performance. Again, there is a need to define a lower threshold on performance to characterize acceptable performance levels. A one kilometer per day increase in the deputy semi-major axis is used as this lower bound. Assuming a circular deputy orbit, the semi-major axis increase in the deputy orbit over one day is (Schaub and Moorer, 2012)

$$\Delta a \approx \frac{4\pi}{n^2}\frac{F_c}{m_D}, \tag{12}$$

where n is the mean motion of the deputy orbit and m_D the deputy mass. A GEO orbit radius of 42,164 km is assumed for this analysis. The deputy mass is required to compute the semi-major axis change. Considering publicly available data on GEO satellites, Schaub and Jasper (2013) provides a relationship between spacecraft mass and an approximate sphere radius. The simple linear expression

$$r_D(m_D) = 1.152\ \text{m} + 0.00066350\ \frac{\text{m}}{\text{kg}} m_D \tag{13}$$

provides a deputy radius for use in the charging model. While certainly not perfect, this linear relationship does capture the general trend of increased mass for larger objects and is based on actual data for GEO objects.

Considering a tug size of $r_T = 3$ meters and an electron beam energy of 40 keV, the semi-major axis increase over one day for a range of deputy sizes is shown in Fig. 6.

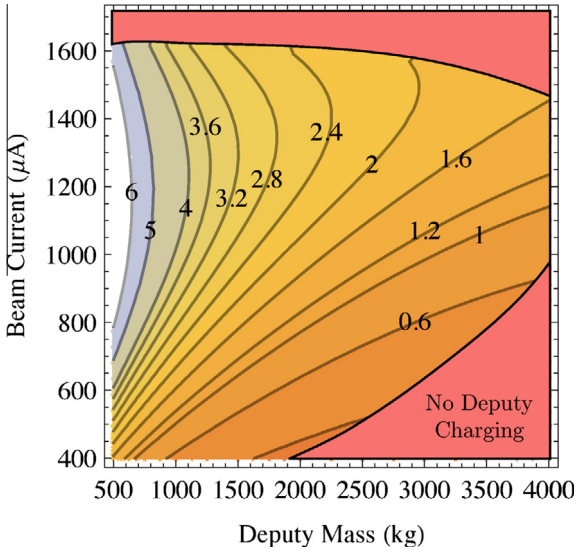

Fig. 6. Deputy semi-major axis increase per day (in km) for a range of deputy sizes and electron beam currents. The tug size is $r_T = 3$ m.

Again, there are two distinct regions of the plot, which correspond to successful charge transfer and no charge transfer. Using charge transfer the 3 m tug can tow objects in excess of 4000 kg faster than the $\Delta a = 1$ km/day threshold. In fact, the maximum rate of increase in the semi-major axis for the 4000 kg objects is about 1.6 km/day. Objects of slightly less than 3000 kg can be towed at $\Delta a = 2$ km/day; reaching a 3 km/day performance level is possible for objects as large as 1700 kg.

4. Power considerations

All of the results regarding limitations on tug and deputy sizing highlight the challenges of tugging a deputy object larger than the tug. There are no issues achieving charge transfer when the deputy is much smaller than the tug ($r_D/r_T \ll 1$). On the contrary, charge transfer and tugging performance in general suffer when the deputy is significantly larger than the tug. This implies that the tug vehicle should be made as large as possible in order to maximize the range of objects that can be towed. Of course, there are tradeoffs to using a larger tug that must be considered. A larger tug vehicle, owing to its larger surface area, will require significantly more current to achieve a desired potential, and this current increases with the square of the tug radius. This means that doubling the tug radius will require four times as much power to achieve supercharging for a given potential. The expression

$$P_{\max} = I_{t,\max} E_{EB} \tag{14}$$

provides the power required for supercharging a tug vehicle ($q\phi_T = E_{EB}$). The variable $I_{t,\max}$ is the maximum current that may be emitted for the given beam energy and is computed as $I_{t,\max} = -I_e(E_{EB})$. Note that this serves as an upper bound on the required power, because the is the maximum amount of current that the tug can emit. Charge transfer generally requires a lower amount of current. The power required to supercharge tug sizes of 1, 2, and 3 m is presented in Fig. 7. Even for the largest 3 m radius tug considered here, power levels of no more than 100 W are required for electron beams of around 50 keV or less.

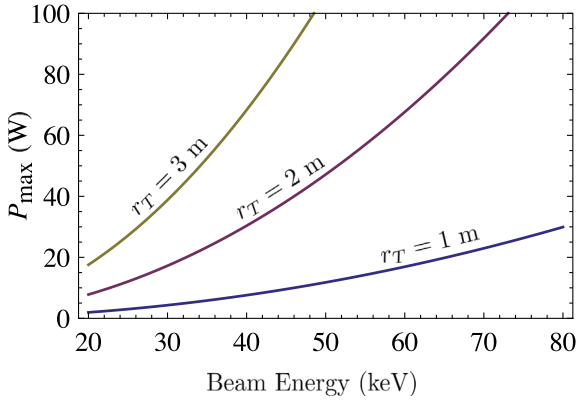

Fig. 7. Power required to supercharge tug vehicle as a function of beam energy.

5. Conclusion

In this study, the impacts of relative sizing between a tug and deputy object on electrostatic tractor performance are investigated. Assuming nominal, quiet GEO space weather conditions, an upper limit on the size ratio is determined that still enables charge transfer between tug and deputy. In general, a tug vehicle will be unable to achieve charge transfer onto an object much greater than itself. The electrostatic forces and resulting debris reorbiting performance are also investigated. The results support the notion that a larger tug size allows for the towing of a wider range of deputy sizes, and that charge transfer performance is significantly hindered if the deputy object is too big relative to the tug. If the tug vehicle is small relative to the deputy, it will maximally charge before delivering enough current to the deputy to initiate charging. Power requirements are also identified for the charging levels considered here. For the largest vehicle sizes, no more than 100 W of power are required to achieve charge transfer.

Acknowledgments

The authors would like to thank Zoltan Sternovsky for his input on the charging dynamics.

References

Anderson, P.C., 2012. Characteristics of spacecraft charging in low earth orbit. J. Geophys. Res.: Space Phys. 117 (A7).

Bartels, J., Heck, N.H., Johnston, H.F., 1939. The three-hour-range index measuring geomagnetic activity. Terr. Magn. Atmos. Electricity 44 (4), 411–454.

Bittencourt, J., 2004. Fundamentals of Plasma Physics. Springer-Verlag, New York.

Cho, M., Ramasamy, R., Matsumoto, T., Toyoda, K., Nozaki, Y., Takahashi, M., 2003. Laboratory tests on 110-volt solar arrays in simulated geosynchronous orbit environment. J. Spacecraft Rockets 40 (2), 211–220.

Cho, M., Sumida, T., Masui, H., Toyoda, K., Kim, J.H., Hatta, S., et al., 2012. Spacecraft charging analysis of large geo satellites using muscat. Plasma Sci., IEEE Trans. 40 (4), 1248–1256.

DeForest, S.E., 1972. Spacecraft charging at synchronous orbit. J. Geophys. Res. 77 (4), 651–659.

Denton, M.H., Thomsen, M.F., Korth, H., Lynch, S., Zhang, J.C., Liemohn, M.W., 2005. Bulk plasma properties at geosynchronous orbit. J. Geophys. Res. 110 (A7).

Draine, B.T., Salpeter, E.E., 1979. On the physics of dust grains in hot gas. Astrophys. J. 231 (1), 77–94.

Garrett, H.B., 1981. The charging of spacecraft surfaces. Rev. Geophys. 19 (4), 577–616.

Hogan, E., Schaub, H., 2013. Relative motion control for two-spacecraft electrostatic orbit corrections. AIAA J. Guidance, Control, Dyn. 36 (1), 240–249.

Hogan, E., Schaub, H., 2014. Space weather influence on relative motion control using the touchless electrostatic tractor. In: AAS/AIAA Spaceflight Mechanics Meeting. Santa Fe, New Mexico (Paper AAS 14–425).

IADC space debris mitigation guidelines, 2007. Tech. Rep. IADC-02-01; Inter-Agency Space Debris Coordination Committee.

Katz, I., Davis, V., Snyder, D.B., 1998. Mechanism for spacecraft charging initiated destruction of solar arrays in geo. In: 36th AIAA Aerospace Sciences Meeting and Exhibit. AIAA. http://dx.doi.org/10.2514/6.1998-1002.

Lai, S.T., 2012. Fundamentals of Spacecraft Charging. Princeton University Press.

Mullen, E.G., Gussenhoven, M.S., Hardy, D.A., 1986. Scatha survey of high-voltage spacecraft charging in sunlight. J. Geophys. Sci. 91, 1074–1090.

Murdoch, N., Izzo, D., Bombardelli, C., Carnelli, I., Hilgers, A., Rodgers, D., 2008. Electrostatic tractor for near earth object deflection. In: 59th International Astronautical Congress, vol. 29. Glasgow, Scotland.

NASA safety standard: Guidelines and assessment procedures for limiting orbital debris, 1995. Tech. Rep. NSS 1740.14; National Aeronautics and Space Administration.

Pfau, S., Tichy, M., 2001. Low Temperature Plasma Physics: Fundamental Aspects and Applications. Wiley, Berlin.

Schaub, H., Jasper, L.E.Z., 2013. Orbit boosting maneuvers for two-craft coulomb formations. AIAA J. Guidance, Control, Dyn. 36 (1), 74–82.

Schaub, H., Moorer, D.F., 2012. Geosynchronous large debris reorbiter: challenges and prospects. J. Astronaut. Sci. 59 (1&2), 165–180.

Schaub, H., Sternovský, Z., 2013. Active space debris charging for contactless electrostatic disposal maneuvers. In: 6th European Conference on Space Debris. ESOC, Darmstadt, Germany, Paper No. 6b.O-5.

Sickafoose, A.A., Colwell, J., Horányi, M., Robertson, S., 2002. Experimental levitation of dust grains in a plasma sheath. J. Geophys. Res. 107 (A11), SMP 37-1–SMP 37-11.

Slisko, J., Brito-Orta, R.A., 2007. On approximate formulas for the electrostatic force between two conducting spheres. Am. J. Phys. 1998 (4), 352–355.

Smythe, W.R., 1968. Static and Dynamic Electricity, McGraw-Hill.

Stiles, L.A., Seubert, C.R., Schaub, H., 2012. Effective coulomb force modeling in a space environment. In: AAS Spaceflight Mechanics Meeting. Charleston, South Carolina. (Paper AAS 12).